

JGR Space Physics

RESEARCH ARTICLE

10.1029/2023JA031325

Key Points:

- We report unambiguous banded signatures of plasmaspheric hiss, uniquely characterized by an upper band above ~200 Hz, a lower band below ~100 Hz and a power gap in between
- Banded plasmaspheric hiss occurs with the probability ~8% in the postnoon sector within 2.5–5.0 Earth radii, showing strong dependence on geomagnetic and solar wind conditions
- Observations suggest that banded hiss waves result from two combined sources, which however requires further investigation

Correspondence to:

B. Ni, D. Summers and Z. Xiang,
bbni@whu.edu.cn;
dsummers@mun.ca;
xiangzheng@whu.edu.cn;












Citation:

Ni, B., Summers, D., Xiang, Z., Dou, X., Tsurutani, B. T., Meredith, N. P., et al. (2023). Unique banded structures of plasmaspheric hiss waves in the Earth's magnetosphere. *Journal of Geophysical Research: Space Physics*, 128, e2023JA031325. <https://doi.org/10.1029/2023JA031325>

Received 16 JAN 2023

Accepted 25 FEB 2023

Unique Banded Structures of Plasmaspheric Hiss Waves in the Earth's Magnetosphere

Binbin Ni^{1,2} , Danny Summers³, Zheng Xiang¹ , Xiankang Dou^{1,4} , Bruce T. Tsurutani⁵ , Nigel P. Meredith⁶ , Junhu Dong¹, Lunjin Chen⁷, Geoffrey D. Reeves^{8,9}, Xu Liu⁷ , Xin Tao¹⁰ , Xudong Gu¹ , Xin Ma¹ , Juan Yi¹ , Song Fu¹ , and Wei Xu¹

¹Department of Space Physics, School of Electronic Information, Wuhan University, Wuhan, China, ²Chinese Academy of Sciences Center for Excellence in Comparative Planetology, Hefei, China, ³Department of Mathematics and Statistics, Memorial University of Newfoundland, St. John's, Newfoundland, Canada, ⁴Chinese Academy of Sciences Key Laboratory of Geospace Environment, University of Science and Technology of China, Hefei, China, ⁵Jet Propulsion Laboratory, California Institute of Technology, Pasadena, CA, USA, ⁶Space Weather and Atmosphere Team, British Antarctic Survey, NERC, Cambridge, UK, ⁷William B. Hanson Center for Space Sciences, University of Texas at Dallas, Richardson, TX, USA, ⁸Space Science and Applications Group, Los Alamos National Laboratory, Los Alamos, NM, USA, ⁹Space Sciences Division, New Mexico Consortium, Los Alamos, NM, USA, ¹⁰Department of Geophysics and Planetary Sciences, University of Science and Technology of China, Hefei, China

Abstract Plasmaspheric hiss is an electromagnetic wave mode that occurs ubiquitously in the high-density plasmasphere and contributes crucially to the dynamic behavior of the Earth's Van Allen radiation belts. While plasmaspheric hiss is commonly considered to be a broadband emission with frequencies from ~100 Hz to several kHz, here we report Van Allen Probes measurements of unambiguous banded signatures of plasmaspheric hiss, uniquely characterized by an upper band above ~200 Hz, a lower band below ~100 Hz and a power gap in between. Banded plasmaspheric hiss occurs with the probability ~8% in the postnoon sector within 2.5–5.0 Earth radii, showing strong dependence on geomagnetic and solar wind conditions. Observations also suggest that banded hiss waves result possibly from two combined sources, the upper band originating from the transformation of chorus waves propagating from outside the plasmasphere, and the lower band from localized excitation inside the plasmasphere, which however requires future investigation. The banded hiss waves shed new light on the evolution of the Earth's radiation belts and have implications for understanding whistler-mode waves in planetary magnetospheres.

1. Introduction

Since the discovery of the Van Allen radiation belts over 60 years ago (Van Allen, 1959), their dynamic variability has been understood to be the result of interactions with a variety of space plasma waves (Summers et al., 2007a; Shprits et al., 2008; Thorne, 2010; W. Li & Hudson, 2019). In particular, plasmaspheric hiss is found to play a critical role in governing the structure and dynamics of the radiation belts. By removing the population of energetic electrons encircling Earth's magnetosphere into the atmosphere on timescales of days or less (Abel & Thorne, 1998; Falkowski et al., 2017; Ni et al., 2013; Summers et al., 2007b; Tsurutani et al., 2019), plasmaspheric hiss can account predominantly for the formation of the radiation belt slot (Falkowski et al., 2017; Lyons & Thorne, 1973; Lyons et al., 1972; Meredith et al., 2007; Tsurutani et al., 1975, 2019), the region between the inner and outer radiation belts where high-energy electron fluxes are typically low. Further, plasmaspheric hiss contributes to electron loss during geomagnetic storms (Lam et al., 2007; Smith et al., 1974; Summers et al., 2007a, 2007b) and the quiet-time decay of outer radiation belt electrons (Meredith, Horne, Glauert, et al., 2006). By means of an energy-dependent scattering process, plasmaspheric hiss generates the reversed electron energy spectrum frequently observed in the plasmasphere (Ni et al., 2019; Zhao et al., 2019). Hiss waves in plasmaspheric plumes can also cause significant scattering loss of energetic electrons in Earth's inner magnetosphere (Summers et al., 2008; Tsurutani et al., 2015).

As a natural constituent of planetary magnetospheric plasma, hiss waves were discovered with the advent of high-altitude satellites (Dunckel & Helliwell, 1969; Russell et al., 1969; Smith et al., 1974; Thorne et al., 1973), and have been historically defined as an electromagnetic emission band between ~100 Hz and 2 kHz (Abel & Thorne, 1998; Meredith, Horne, Glauert, et al., 2006; Ni et al., 2013; Summers et al., 2007a, 2007b; Tsurutani et al., 2015; Zhao et al., 2019). This emission occupies Earth's plasmasphere or detached plas-

maspheric plumes, and makes a hissing sound when played through a loudspeaker. Notwithstanding over 50 years of observations, the origin of plasmaspheric hiss remains controversial (Bortnik et al., 2016; Green et al., 2005, 2006; Hartley et al., 2019; Rodger & Clilverd, 2008; Santolik & Chum, 2009; Santolik et al., 2021; Thorne et al., 2006). Three distinct generation mechanisms have been put forward: (a) in situ cyclotron resonance wave instability driven by electron anisotropy (Thorne et al., 1979, 2006; Church and Thorne, 1983; Meredith et al., 2004; Meredith, Horne, Clilverd, et al., 2006), (b) lightning-generated whistlers leaking into the plasmasphere (Draganov et al., 1992; Green et al., 2005; Santolik et al., 2021; Sonwalkar & Inan, 1989), and (c) refraction of chorus waves propagating into the plasmasphere (Bortnik et al., 2016; Chum & Santolik, 2005; Falkowski et al., 2017; Rodger & Clilverd, 2008; Santolik & Chum, 2009; Santolik et al., 2006; Tsurutani et al., 2015, 2019). The major characteristics of traditionally observed hiss and its dependence on solar wind-driven magnetospheric compression may be explained from chorus waves as the embryonic source (Bortnik et al., 2008, 2009, 2011; Meredith et al., 2013; Tsurutani et al., 2015). However, the relative contribution of each of the different mechanisms to the formation of plasmaspheric hiss is still an open question (Bortnik et al., 2016; Hartley et al., 2019; Meredith et al., 2021; Rodger & Clilverd, 2008; Santolik & Chum, 2009, 2021) that requires further high-quality measurements to answer. Furthermore, relatively recent studies (Nakamura et al., 2018; Summers et al., 2014) have revealed that whistler mode hiss is a coherent emission with complex fine structure consisting of discrete rising tone and falling tone elements. Such fine structure would appear to strengthen the assertion that the dominant hiss generation mechanism is the electron cyclotron resonance instability occurring near the magnetic equator, though further analysis is required to unquestionably establish this argument.

2. Data and Methodology

2.1. Determination of an Observation Inside or Outside the Plasmasphere

Since plasmaspheric hiss can overlap in frequency with other magnetospheric waves such as whistler-mode chorus, the determination of an observation inside/outside the plasmasphere or the plasmopause location is key to distinguish between these two wave modes. There are two methods to identify a plasmopause crossing: one is to follow the definition of the plasmopause as the boundary layer where the ambient plasma density varies by a factor ≥ 5 within a radial distance of $0.5 L$ (Moldwin et al., 2002); the other is to adopt the presence or absence of electrostatic electron cyclotron harmonic (ECH) waves as a proxy to determine whether a particular observation is outside or inside the plasmopause (Meredith et al., 2004; Meredith, Horne, Clilverd, et al., 2006), because ECH waves occur characteristically in the low-density plasmatrough (Liu et al., 2020).

In our analysis, high frequency receiver (HFR) data from the Van Allen Probes EMFISIS instrument can provide both the information of ambient plasma density extracted based on the traces of upper hybrid resonance frequency (Kurth et al., 2015) and the electric field spectral intensities covering the ECH wave frequencies. The data of HFR wave spectral intensities are continuously available, while the data of ambient plasma density have gaps at times. Consequently, in order to facilitate our statistical investigation of the occurrence properties of banded plasmaspheric hiss, we use the method based on the ECH wave intensity (Meredith et al., 2004; Meredith, Horne, Clilverd, et al., 2006) to determine whether an observation is located inside or outside the plasmopause. Specifically, if the ECH wave electric field amplitude, calculated as the square root of the integrated spectral intensity in the first harmonic band ($f_{ce} < f < 2f_{ce}$), is less than or greater than 0.0005 mV/m (Meredith et al., 2004), the particular observation is considered to be inside or outside the plasmasphere, respectively. The transition location between these two regions are then determined as the position of the plasmopause. At higher L -shells, the electron gyrofrequency decreases, and higher-order harmonic bands rather than the first harmonic band of ECH waves become observable. Then we select the HFR power spectral data at a fixed frequency range for further consideration (Ma et al., 2016), for instance, $1-4 f_{ce}$ for $L = 3.5-4.5$, $1-6 f_{ce}$ for $L = 4.5-5.5$, and $1-8 f_{ce}$ for $L > 5.5$. If the lower limit of this range is lower than the lower frequency limit of the HFR, say, 10 kHz , we take 10 kHz as the lower limit. If the upper limit of this range is higher than 500 kHz (The upper limit frequency of HFR data), we take 500 kHz as the upper limit. We then take 80% of the peak spectral intensity in the above frequency range as the threshold value. If this value is larger than $10^{-16} (\text{V/m})^2/\text{Hz}$ or 5 times the background noise level, we decide that the observation is outside the plasmasphere. Otherwise, we determine that the observation is inside the plasmasphere. When the information of ambient plasma density is also available, we implement the above two methods to identify the plasmopause location, the results of which generally show good agreement.

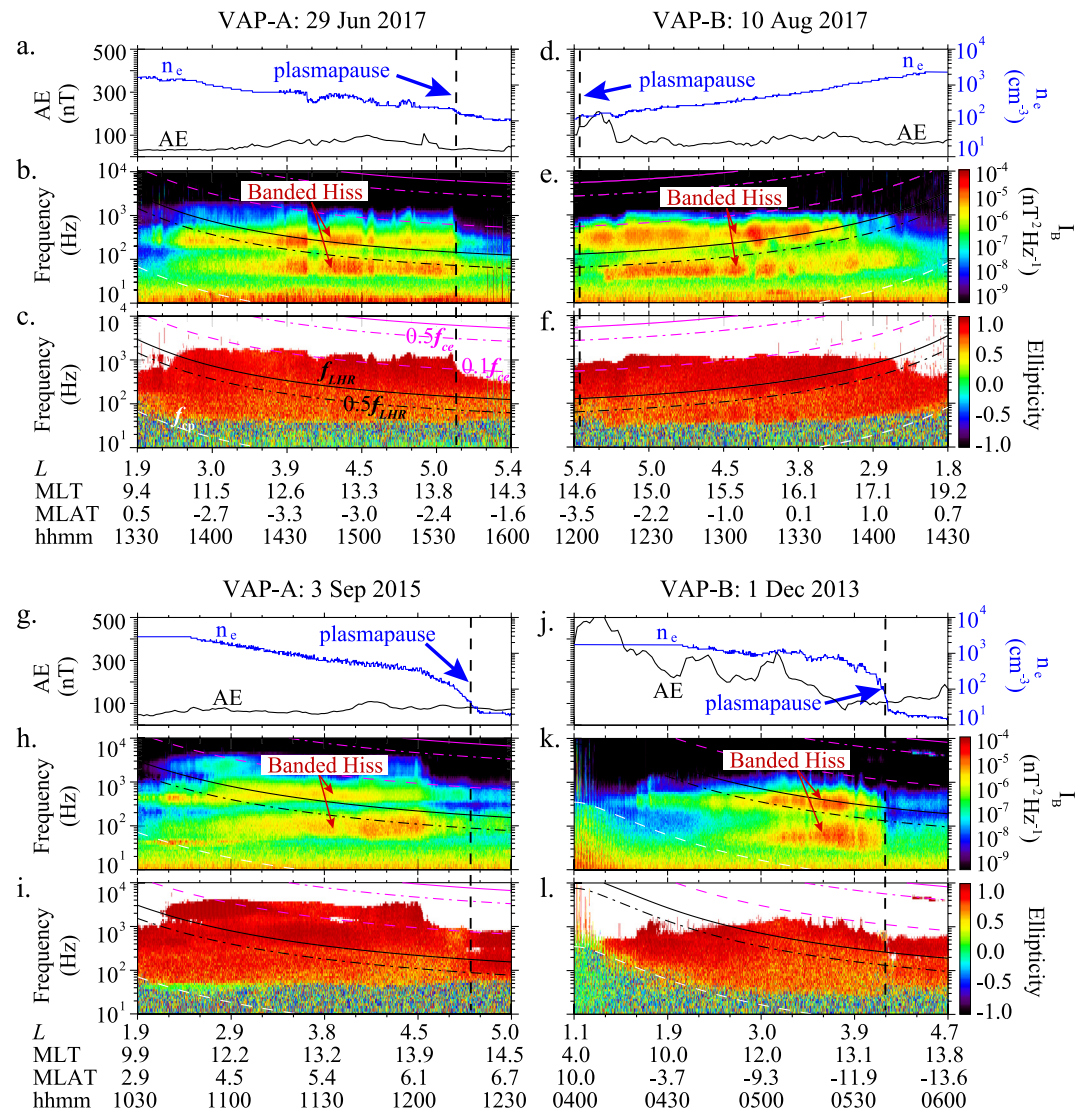


Figure 1. Observations of banded plasmaspheric hiss by the twin Van Allen Probes (VAP) EMFISIS instrument. Four representative banded plasmaspheric hiss events occurred, respectively, on (a–c) 29 June 2017, (d–f) 10 August 2017, (g–i) 3 September 2015, and (j–l) 1 December 2013. (a, d, g, j) Temporal variations of the geomagnetic auroral electrojet (AE) index and of the ambient electron density (n_e). The vertical dashed line in each panel denotes the plasmapause location. (b, e, h, k) Spectrograms of magnetic field wave power (I_B) for the banded plasmaspheric hiss waves observed inside the plasmapause; L value calculated using the Olson-Pfizer external magnetic field model (Olson & Pfizer, 1977) and the IGRF internal field model (Finlay et al., 2010), magnetic local time (MLT), magnetic latitude (MLAT), and time of measurements are also shown. The over-plotted color-coded curves, from top to bottom, represent the electron gyrofrequency (f_{ce}), $0.5f_{ce}$, $0.1f_{ce}$, the lower hybrid resonance frequency (f_{LHR}), $0.5f_{LHR}$, and the proton gyrofrequency (f_{cp}). (c, f, i, l) Detailed information of the ellipticity as a function of wave frequency for the banded plasmaspheric hiss events.

2.2. Identification of Banded Plasmaspheric Hiss Wave Events

Using wave datasets with fine frequency resolution from the Electric and Magnetic Field Instrument Suite and Integrated Science (EMFISIS) instrument (Kletzing et al., 2013) onboard the Van Allen Probes (Mauk et al., 2013), we observe a unique class of hiss waves in the plasmasphere, consisting of two distinct frequency bands with a power gap in between and therefore termed banded plasmaspheric hiss. Figure 1 shows four representative examples of banded plasmaspheric hiss identified unambiguously inside the plasmapause (the outermost boundary of the plasmasphere). On the basis of the spectrograms for each event (Figures 1b, 1e and 1h, 1k), the key common features of this remarkable emission include a frequency spectral profile characteristic of an upper band, a lower band and a gap, a close correlation of wave power with the plasmapause location and plasma density (Figures 1a,

1d and 1g, 1j), and the dominance of right-handed polarization (Figures 1c, 1f and 1i, 1l). The upper band and lower band waves are measured over the frequency range of ~ 200 – $1,000$ Hz and ~ 40 – 150 Hz, respectively, with a gap in frequency corresponding to the power minimum at ~ 150 – 200 Hz. Both bands exhibit power spectral densities at a similar level, and can last over an hour to occupy a broad spatial region of L -shell (where L is the geocentric distance in Earth radii of the location at which a dipolar magnetic field line crosses the geomagnetic equator). Clearly, banded plasmaspheric hiss can be observed from the geomagnetic equator (Figure 1e) to the magnetic latitude $\sim 12^\circ$ (Figure 1k) during periods of either quiet or disturbed geomagnetic activity (see the profiles of the geomagnetic Auroral Electrojet index AE).

Since plasmaspheric hiss can overlap in frequency with other magnetospheric waves such as whistler-mode chorus, the determination of an observation inside/outside the plasmasphere or the plasmopause location is key to distinguish between these two wave modes. Along with the determination of an observation revealing a location as inside or outside the plasmasphere, we establish a robust identification criterion to determine the events of banded plasmaspheric hiss:

1. We focus on the wave frequency range of 20–10000 Hz with the wave magnetic field spectral intensities larger than 10^{-8} nT²/Hz. Selection of such a broad frequency band guarantees the entire coverage of banded plasmaspheric hiss frequencies. Further, our choice of the above background noise threshold of the Van Allen Probes search coil magnetometers (SCM) ensures that all the values above this threshold for the wave power at >100 Hz correspond to real geophysical signals rather than SCM noises (Hospodarsky, 2016; Malaspina et al., 2017). For hiss waves below 100 Hz, although the fixed threshold may identify falsely some SCM noises as real signals (Malaspina et al., 2017), the relative percentage of these events is overall small ($<\sim 10\%$) and hence will not affect the following analysis much.
2. We focus on the wave emissions with the ellipticity larger than 0.5, which is calculated using the singular value decomposition (SVD) method (Santolik et al., 2003). As a key feature of whistler-mode waves (Verkhoglyadova et al., 2010), the dominance of right-handed polarization can finely distinguish plasmaspheric hiss waves from magnetosonic waves that may overlap in frequency with the former.
3. We specify that the ratio between the peak frequencies of the upper band and lower band emissions should be larger than 2.5, that is, $f_{UP}/f_{LP} > 2.5$. By doing so, we ensure that the frequency separation is large enough to distinguish the individual bands of plasmaspheric hiss.
4. We specify that the ratio between the wave spectral densities at the peak frequencies of the two bands should be within a factor of 4, that is, $0.25 < I_B(f = f_{UP})/I_B(f = f_{LP}) < 4.0$. In this way, we can remove the events that appear to be two-band emissions but are substantially dominated by one band. Thus, we concentrate on events of banded plasmaspheric hiss that exhibit clear signatures of two peaks of wave spectral intensity at the comparable level. While this choice may conservatively omit some banded plasmaspheric hiss events, it ensures that all the identified plasmaspheric hiss events bear unambiguous twin bands rather than one band.
5. We specify that the ratio between the wave spectral densities at the lower-band peak frequency and the gap frequency should be larger than 2.5, that is, $I_B(f = f_{LP})/I_B(f = f_{gap}) > 2.5$. By doing so, we ensure that the emission between the two wave intensity peaks clearly exhibits a minimum in wave power to form the banded structure.
6. We specify in this investigation that an event of banded plasmaspheric hiss should last continuously for at least 10 min. By removing those events with the shorter time duration, we guarantee that each event of banded plasmaspheric hiss is rigorously identified.

Following the entire procedure described above, we investigate the Van Allen Probes EMFISIS datasets spanning the period from 15 September 2012 to 30 June 2019 to establish a robust database of banded plasmaspheric hiss. This database consists of 2,616 cases of banded plasmaspheric hiss, corresponding to 649,223 data points in total and representing good spatial coverage (see Figure 2).

3. Spectral Characteristics and Occurrence Pattern of Banded Plasmaspheric Hiss

As illustrated in Figure 3a, two peak wave frequencies and one gap frequency coexist to form banded plasmaspheric hiss. The established database of banded plasmaspheric hiss waves based on ~ 7 years of Van Allen Probes EMFISIS measurements enables our detailed analyses of their spectral characteristics and occurrence pattern.

The averaged power spectral densities of all identified events (Figure 3b) clearly reveal the characteristic nature of a banded hiss profile. Statistically, the gap frequency (f_{gap}) is mostly present at 100–250 Hz (Figure 3d) with an

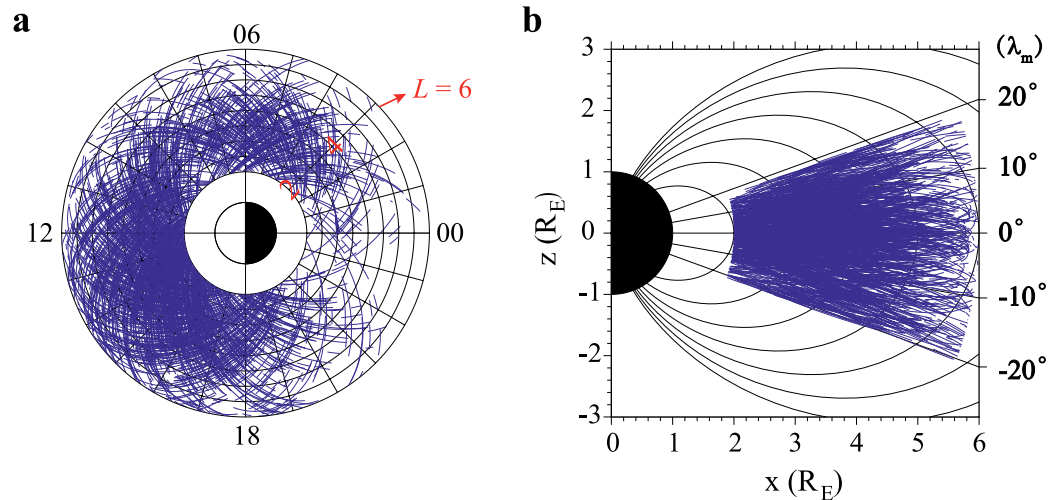


Figure 2. Van Allen Probes trajectories corresponding to the database of banded plasmaspheric hiss events. In total, 2,616 cases of banded plasmaspheric hiss are identified from ~ 7 years of the EMFISIS datasets. (a) (L, MLT) -map of the event distribution in the equatorial plane, and (b) (L, MLAT) -map of the event distribution in the meridian plane, both showing good spatial coverage for statistical investigation.

occurrence probability $\sim 70\%$ (Figure 3g). The peak wave frequency for the lower band (f_{LP}) is observed typically at 50–150 Hz (Figure 3c) with a probability $\sim 80\%$ (Figure 3f). The peak wave frequency for the upper band (f_{UP}) commonly occurs at 250–400 Hz (Figure 3e) with a rate $\sim 60\%$ (Figure 3h).

The majority of banded plasmaspheric hiss events occur in the region $L \sim 2.5\text{--}5.0$ (Figures 3b–3e) with the largest occurrence rate of $\sim 8\%$ in the magnetic local time (MLT) sector $\sim 12\text{--}17$ (Figures 4g–4i). As the level of geomagnetic activity (denoted by the index AE^* on the top) increases, the most probable location of banded plasmaspheric hiss gradually shrinks, and shifts toward the prenoon sector and lower L -shells, which is consistent with the dynamic of the plasmapause (Malaspina et al., 2016; Ripoll et al., 2022). Banded plasmaspheric hiss also occurs with a strong dependence on solar wind dynamic pressure (P_{dyn}). When P_{dyn} is high, the occurrence probability can reach $\sim 10\%$ at $L \sim 2.5\text{--}3.5$ and $\text{MLT} \sim 12$, but its peak decreases and moves to the postnoon sector at higher L -shells for $P_{\text{dyn}} \leq 3$ nPa (Figures 4q–4r). The average wave amplitudes (B_w) of the upper band and lower band of banded hiss show a similar global distribution and clear variability with respect to geomagnetic activity (Figures 4a–4f). Corresponding to enhanced levels of geomagnetic disturbance, both bands intensify with the peaks in the wave amplitude gradually shifting from the postnoon sector to the prenoon sector. As P_{dyn} increases, the peak amplitudes of both bands vary slightly and occur at lower L -shells in a narrow postnoon sector (Figure 4m–4p). While the intensities of both bands can be comparable in some events (Figure 1), the amplitude of lower band hiss on average is smaller than that of upper band hiss by a factor $>> 3$. Specifically, while increasing with enhanced geomagnetic activity and solar wind dynamic pressure, the averaged wave amplitude varies mostly within 10–100 pT for the upper band of banded hiss and within a few pT to 30 pT for the lower band. Overall, banded plasmaspheric hiss is preferentially confined to the postnoon-side plasmasphere (Malaspina et al., 2017; Meredith et al., 2021; Tsurutani et al., 2019), and largely dependent on geomagnetic activity and the solar wind conditions.

4. Plausible Mechanisms Responsible for the Generation of Banded Plasmaspheric Hiss

The nature of banded plasmaspheric hiss provides basic clues as to the origin of this wave mode. Since the gap frequency of banded hiss waves tend to be close to the typical $0.5 f_{ce}$ frequency gap of chorus waves, it is natural to propose that banded chorus waves propagate into the plasmasphere to become banded plasmaspheric hiss. However, the gap frequency of banded hiss is generally around 100–250 Hz, which corresponds to the value of $0.5 f_{ce}$ at $L > \sim 12$. Chorus waves at such high L -shells would be substantially attenuated by Landau damping before reaching the plasmasphere due to long raypaths (Chen et al., 2014). Thus, banded hiss waves are unlikely to originate directly from chorus outside the plasmasphere. In addition, since the gap frequency of banded plasmaspheric hiss varies only slightly over a broad range of L -shell, the power minimum between the upper band and lower band cannot be readily attributed to the sole mechanism of local cyclotron absorption or Landau damping. This is because these processes rely mostly on the profiles of the geomagnetic field, ambient plasma density and the energetic particle distribution

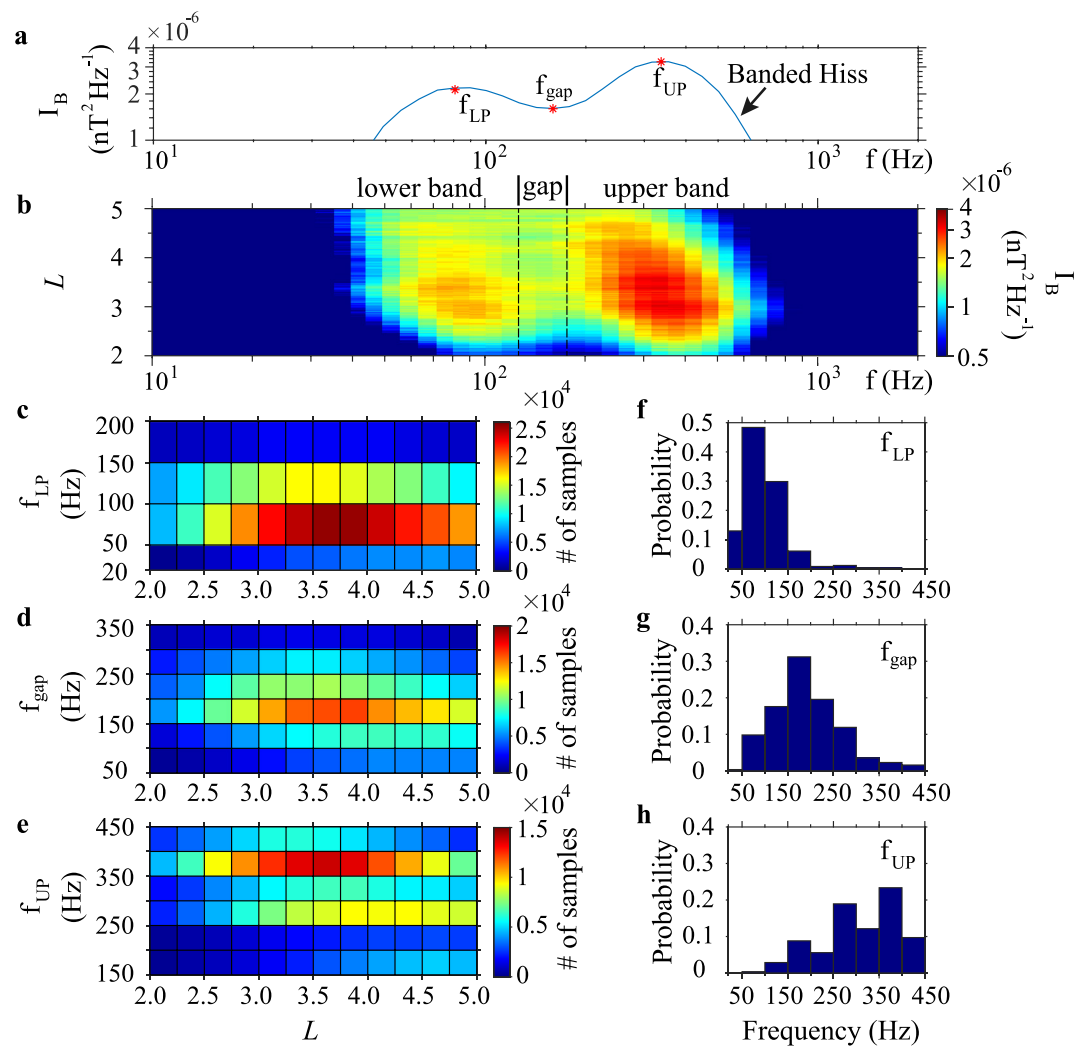


Figure 3. Features of the frequency spectrum of banded plasmaspheric hiss. (a) A statistical plot at $L = 3$ showing a general frequency profile of banded plasmaspheric hiss characterized by two peak wave frequencies and the power gap in between. (b) Averaged power spectral intensities of banded plasmaspheric hiss as a function of wave frequency and L -shell on the basis of a robust event database established using Van Allen Probes EMFISIS wave data spanning the period 2012–2019. (c–e) Number distributions of the three characteristic wave frequencies (f_{LP} and f_{UP} , the peak frequencies for the lower and upper bands, respectively; f_{gap} , the frequency corresponding to the power minimum between the two bands) in the specified (L , frequency)-bins. (f, g, h) Histograms of the occurrence probability of f_{LP} , f_{gap} and f_{UP} in different frequency bins, calculated as the ratio between the sample number in each frequency bin and the number of all the samples.

(Bortnik et al., 2006; Chen et al., 2012c; J. Li et al., 2019; Kennel & Petschek, 1966; Tsurutani et al., 1979). Further, the pronounced correlation of banded plasmaspheric hiss wave occurrence with geomagnetic activity and solar wind dynamic pressure (Figure 4) strongly implies a non-lightning source and points to natural instabilities in the magnetosphere (Meredith, Horne, Clilverd, et al., 2006; Meredith et al., 2004; Smith et al., 1974; Thorne et al., 1973, 2006; Tsurutani et al., 2015). In principle, unstable distributions of energetic electrons at different energies supply the free energy to trigger the wave excitation at different frequencies (Kennel & Petschek, 1966). Correspondingly, following the gyroresonant wave-particle interaction condition and computing the minimum electron resonant energies (e.g., Ni & Summers, 2010; Summers et al., 2007a), the upper band plasmaspheric hiss centered at ~ 250 – 400 Hz is likely to interact with electrons at energies ~ 20 – 100 keV, while the lower band plasmaspheric hiss centered at ~ 50 – 150 Hz is likely to resonate with electrons at several hundreds of keV (see Figure 5). Therefore, the nature of the observed twin-band structure of plasmaspheric hiss renders more likely twin generation mechanisms rather than one.

A plausible two-source scenario for banded plasmaspheric hiss is that the upper band originates from the transformation of chorus waves propagating from outside the plasmasphere (e.g., Bortnik et al., 2008, 2009; Li, Chen

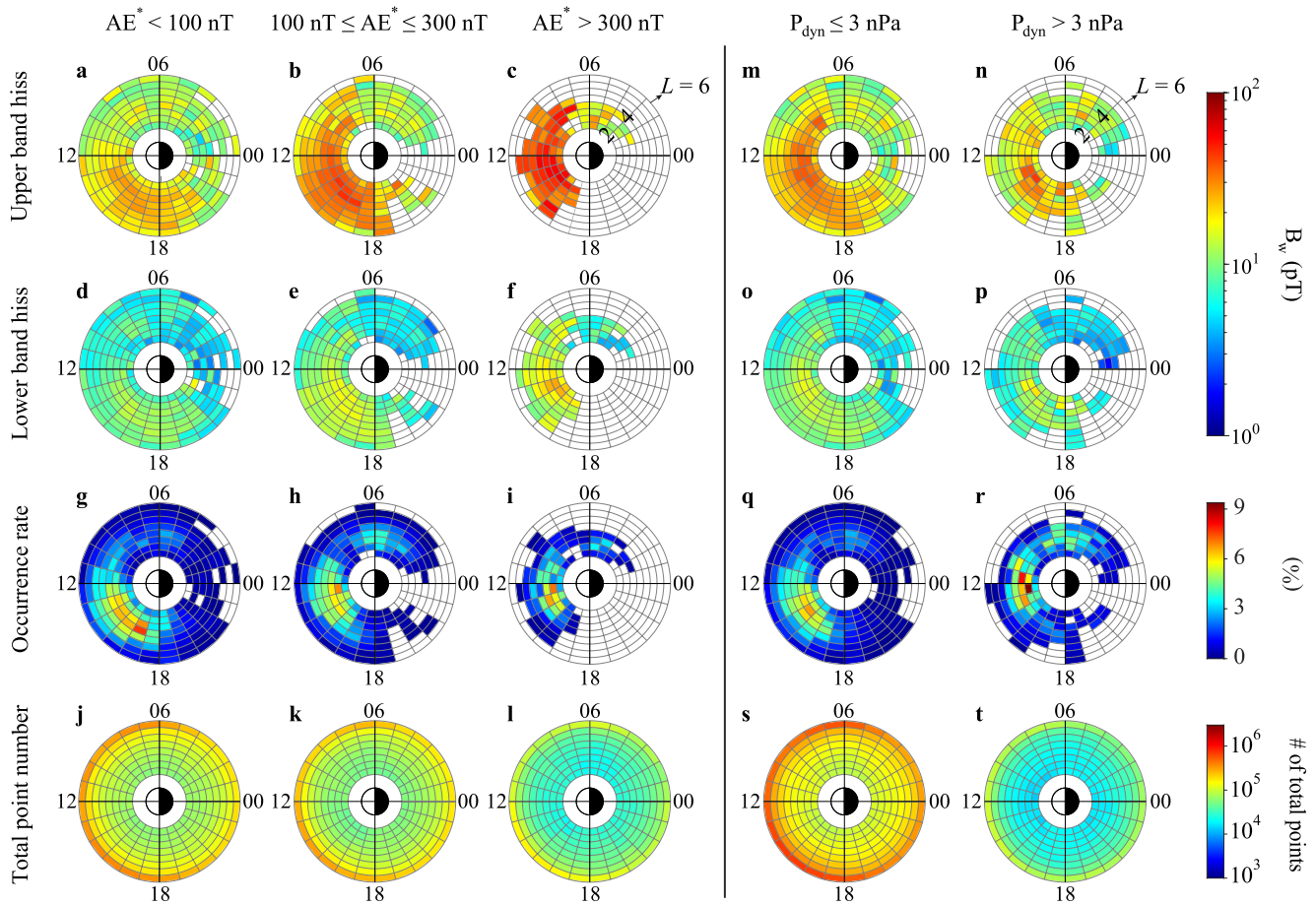


Figure 4. Global distributions of banded plasmaspheric hiss with respect to geomagnetic activity and solar wind dynamic pressure. The intensity of geomagnetic disturbance is categorized into three levels: quiet ($AE^* < 100 \text{ nT}$), moderate ($100 \text{ nT} \leq AE^* \leq 300 \text{ nT}$) and strong ($AE^* > 300 \text{ nT}$), according to the average values of AE in the previous three hours (AE^*). The intensity of solar wind dynamic pressure (P_{dyn}) is categorized into two levels: $P_{\text{dyn}} \leq 3 \text{ nPa}$ and $P_{\text{dyn}} > 3 \text{ nPa}$. Global maps of the statistically averaged wave amplitude (B_w) for upper band and lower band plasmaspheric hiss as a function of L and MLT under (a–f) the three geomagnetic conditions and (m–p) the two solar wind dynamic pressure conditions. Corresponding to the two categories of AE^* and P_{dyn} , the global distributions of all the data points are shown in (j–l) and (s, t), and the global distributions of the occurrence rate of banded plasmaspheric hiss are shown in (g–i) and (q, r), respectively. The data gaps in the (L , MLT)-maps are attributed to either the coverage of satellite trajectories under different AE^* and P_{dyn} conditions or the spatial distribution of banded hiss observations.

et al., 2015) and the lower band from localized excitation inside the plasmasphere (Chen et al., 2014; Li et al., 2013) (Figure 6c). The upper band plasmaspheric hiss has a favorable frequency correlation with whistler-mode chorus occurring outside the plasmasphere. Mainly generated by unstable electron distributions of energy $\sim 1\text{--}100 \text{ keV}$ (Lam et al., 2010; J. Li et al., 2019; Tsurutani et al., 1979), chorus can extend to high latitudes primarily in the prenoon sector (Tsurutani & Smith, 1977; Tsurutani et al., 2009). Dayside chorus emissions can access the plasmasphere in both the prenoon sector and, by means of off-meridional propagation, the postnoon sector to evolve into plasmaspheric hiss (Agapitov et al., 2018; Bortnik et al., 2008, 2009, 2011; Chen et al., 2009, 2012b; Meredith et al., 2013, 2021). As the geomagnetic activity or solar wind dynamic pressure intensifies, dayside chorus can also be generated and amplified in association with minimum magnetic field pockets so that the waves travel a shorter distance to the plasmapause to undergo less damping and greater plasmaspheric intensities (Tsurutani et al., 2012). These associations between chorus and hiss are in good agreement with our findings of the preferential location of banded hiss in the noon-to-dusk sector and also the associated occurrence dependence (Figures 4g–4i and 4q–4r). This suggests that the upper band of banded hiss could originate from the evolution of chorus waves propagating from outside the plasmasphere (Figure 6a).

In contrast, the lower band of banded hiss is unlikely to originate from chorus, since a rarely observed high ratio between the electron plasma-to-cyclotron frequency in the dayside outer magnetosphere (i.e., the ratio > 20

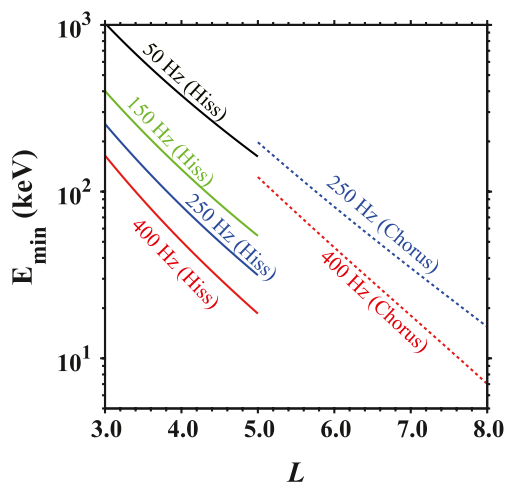


Figure 5. Minimum electron cyclotron resonant energies for plasmaspheric hiss and chorus waves. The dipole magnetic field model and the empirical plasma density model (Sheeley et al., 2001) are adopted to compute E_{\min} for hiss at $L = 3\text{--}5$ inside the plasmasphere and for chorus at $L = 5\text{--}8$ outside the plasmasphere. The indicated four frequencies are specifically selected to correspond to the observed preference of peak wave frequencies for lower and upper band plasmaspheric hiss (Figures 3f and 3h).

at $L \sim 8$) (W. Li et al., 2013; Shi et al., 2017; Malaspina et al., 2016) is required to generate chorus waves at corresponding low frequencies (down to ~ 20 Hz). These low-frequency chorus waves are also not observed to extend to high latitudes (Meredith et al., 2013). Our observations of banded hiss reveal its peak occurrence in a localized region close to the plasmapause in the afternoon sector (Figures 4g–4i). As the solar wind dynamic pressure increases, banded plasmaspheric hiss shifts toward the noonside and occurs with higher probability (Figures 4q–4r). This infers a connection with enhanced electron instability in the dayside plasmasphere under the impact of magnetospheric compression (W. Li et al., 2013; Tsurutani et al., 2015). Such features support our contention that the lower band of banded hiss originates from a local excitation process through the cyclotron resonance instability (Figure 6b). The source electron population may result either from the azimuthal drift of substorm-injected electrons from the nightside to the dayside (W. Li et al., 2013; Shi et al., 2017; Malaspina et al., 2017) or from cross-field diffusion into the dayside plasmasphere by intense dayside chorus generated in minimum magnetic field pockets (Tsurutani & Thorne, 1982). Our observations also reveal the extension of lower band of banded hiss down to $L < \sim 3.0$ where the resonant electron energies for low frequency hiss (< 50 Hz) are above 1 MeV (see Figure 5). However, relativistic electrons rarely penetrate into $L < 3$, as observed by Van Allen Probes (e.g., Baker et al., 2014; Li et al., 2015). Thus, it is unlikely that such low frequency hiss is directly generated by an injection of source electrons, but it could possibly be explained by inward wave propagation associated with density gradient

structures (e.g., the plasmapause) (Chen et al., 2012a, 2012c, 2014; Green et al., 2006; Malaspina et al., 2016; Thorne et al., 2006).

Besides the two-source scenario, there may well exist other hypotheses regarding the generation of banded plasmaspheric hiss. It is possible that upper band hiss is locally excited by electrons drift into plasma tails or the plasmaspheric bulge, especially during periods of quiet geomagnetic activity (Figure 4a). In addition, low-frequency whistler waves may be originally triggered on the dayside at minimum magnetic field pockets with low field intensities and then propagate into the plasmasphere to become lower band hiss. Inevitably, the various potential generation scenarios require detailed investigation in follow-up studies.

5. Summary

Banded whistler-mode chorus is very well known to space physicists and has been observed almost from the beginning of the observations of chorus itself in the 1960s (Burtis & Helliwell, 1969, 1976; Meredith et al., 2012; Tsurutani & Smith, 1974). However, banded plasmaspheric hiss has received little focus prior to our present study. Our results, which have been made possible by the excellence of the EMFISIS instrument on the Van Allen Probes mission, are the first to demonstrate that this new type of plasmaspheric hiss has characteristics of the power gap and occurrence pattern distinct from those of banded chorus. Meanwhile, it is worth noting that while the study of Malaspina et al. (2017) showed two events of concurrent lower band and upper band hiss, they examined the statistics of both lower band hiss and upper band hiss without any concentration on the simultaneously occurring banded emissions of hiss waves. Zhu et al. (2019) presented another concurrent event of normal hiss and low-frequency hiss, but they stated that it was a “rare” case and focused on analyzing the observed fine structures of the normal hiss. Although He et al. (2019, 2021) studied so-called “two-band” plasmaspheric hiss waves, what they reported is a combination of normal hiss and higher-frequency (up to 10 kHz) hiss, which is totally different from our reported banded plasmaspheric hiss which is uniquely characterized by an upper band above ~ 200 Hz, a lower band below ~ 100 Hz and a power gap in between. Furthermore, the recent study of Meredith et al. (2021) has claimed that the higher-frequency waves observed above 2 kHz on the dawnside at $L > 4.0$ during active conditions by He et al. (2020) are predominantly chorus waves outside the plasmasphere, indicating that the two-band plasmaspheric hiss events reported by He et al. (2019, 2021) are unlikely to be a kind of two-band emission but more likely two distinct wave modes.

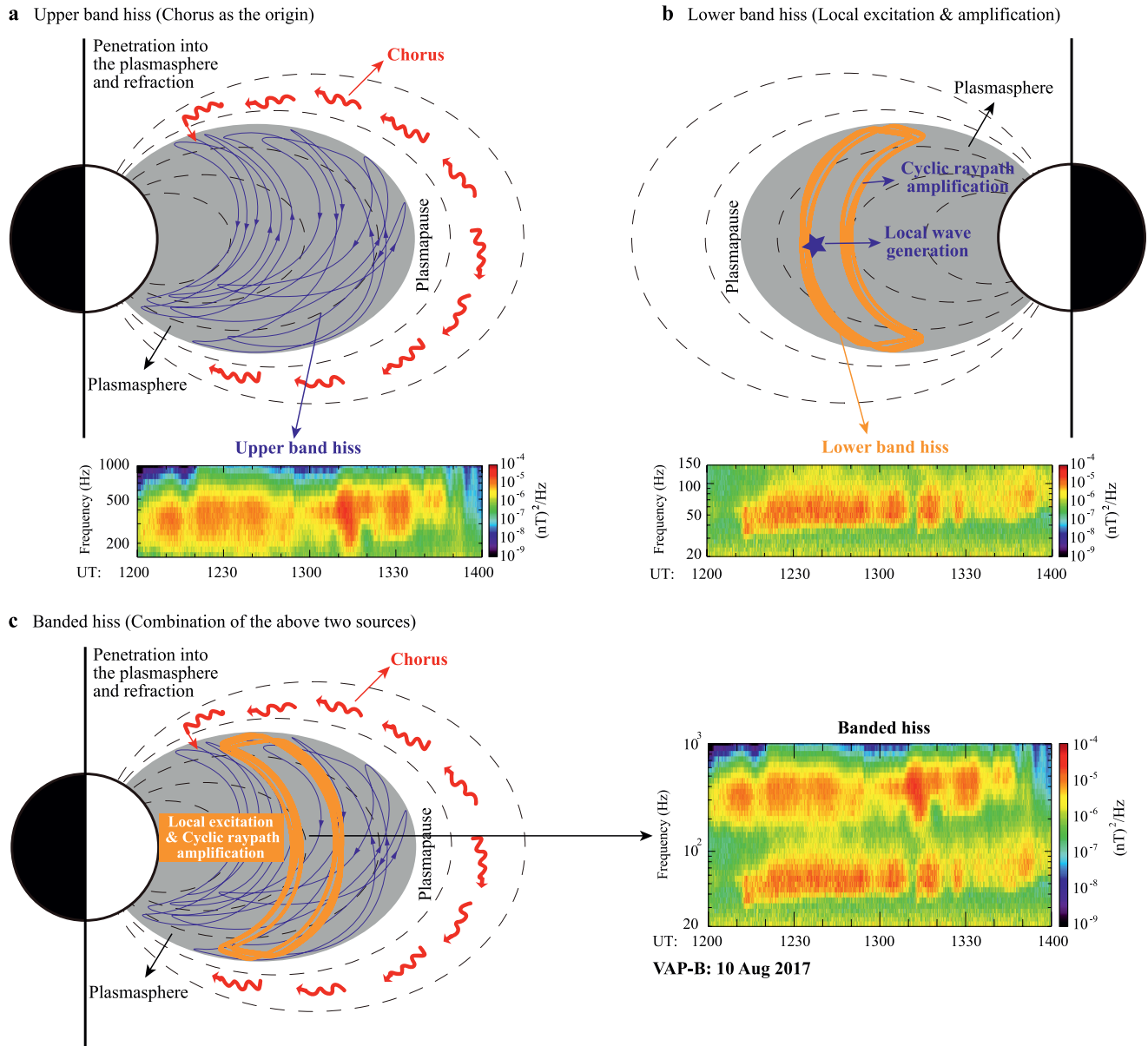


Figure 6. Schematic illustration of a two-source scenario explaining the generation of banded plasmaspheric hiss. a, Evolution of whistler-mode chorus into upper band plasmaspheric hiss on the dayside, by means of penetration from the low-density plasmatrough into the high-density plasmasphere and subsequent refractive superposition inside the plasmasphere. b, Excitation of lower band plasmaspheric hiss due to local cyclotron resonance instability, with the source electron population either drifting azimuthally from the nightside or transporting radially inward on the dayside. Aided by the ambient density gradient associated with the plasmapause, lower band plasmaspheric hiss can undergo cyclic raypaths and repeated amplification in the plasmasphere to yield sufficient net wave gain for growth from the background thermal noise (Chen et al., 2012a, 2014; Green et al., 2006; Thorne et al., 2006). c, Combination of the above two generation mechanisms to form banded plasmaspheric hiss. The three spectrograms, with the duration of about 2 hr on 10 August 2017, exemplify the generation of the observed banded plasmaspheric hiss in terms of this two-source scenario.

Scattering by normal hiss has been found to account for the formation of radiation belt slot (Lyons & Thorne et al., 1973) and the reversed energetic electron energy spectrum (Ni et al., 2019; Zhao et al., 2019). By comparison, low frequency hiss can accelerate the losses of ~50–200 keV electrons and produce more pronounced pancake distributions (Ni et al., 2014). Thus, banded hiss waves reported in this study are likely to combine the scattering effects induced by both normal hiss and low frequency hiss. Because the two hiss bands are expected to cause efficient scattering precipitation of the electron population at different energy ranges (Lyons & Thorne, 1973; Lyons et al., 1972; Tsurutani et al., 1975; Abel & Thorne, 1998; Summers et al., 2007a, 2008; Shprits et al., 2008; Thorne, 2010; Bortnik et al., 2011; Meredith, Horne, Glauert, et al., 2006, 2007; Lam

et al., 2007; Ni et al., 2014, 2019; Breneman et al., 2015; W. Li et al., 2015; Falkowski et al., 2017; Zhao et al., 2019; W. Li & Hudson, 2019; Tsurutani et al., 2019), our findings add new insight into the contributions of plasmaspheric hiss to the variability of the Van Allen radiation belts. While modeling efforts remain to be done to clarify the detailed generation process of banded plasmaspheric hiss, our results also provide plausible evidence to support a combination of two different mechanisms as the origin of banded plasmaspheric hiss: the transformation of chorus waves propagating from outside the plasmasphere, and the local wave instability inside the plasmasphere. In nature, the free energy for banded plasmaspheric hiss originates from unstable distributions of energetic electrons, and creates different instabilities in different locations. Under the impact of solar wind and geomagnetic disturbances, the distinct dynamic behavior and global morphology of the electron population at different energies should overall largely control the generation of upper band and lower band plasmaspheric hiss. The plasmopause location and the ambient profiles of plasma density and magnetic field should also play an important role. Since hiss waves are ubiquitous across planetary magnetospheres and the process of wave-particle interactions is physically universal, our findings have important implications for understanding the complexity of whistler-mode waves and wave-particle energy exchange in planetary magnetospheres more generally.

Data Availability Statement

The Van Allen Probes data from the EMFISIS instrument are obtained from <https://emfisis.physics.uiowa.edu/data/index>; the solar wind and geomagnetic activity indices are publicly available at the NASA OMNIWeb (<http://cdaweb.gsfc.nasa.gov>).

Acknowledgments

This work was supported by the National Natural Science Foundation of China (42025404, 42188101, and 42174190), the National Key R&D Program of China (2022YFF0503700), the B-type Strategic Priority Program of the Chinese Academy of Sciences (XDB41000000), and a Discovery Grant of the Natural Sciences and Engineering Research Council of Canada. We also thank the Van Allen Probes EMFISIS Science Team for providing the wave data, and thank the NSSDC OMNIWeb for the use of solar wind and geomagnetic index data.

References

- Abel, R. W., & Thorne, R. M. (1998). Electron scattering loss in Earth's inner magnetosphere, 1. Dominant physical processes. *Journal of Geophysical Research*, 103(A2), 2385–2396. <https://doi.org/10.1029/97JA02919>
- Agapitov, Q., Mourenas, D., Artemyev, A., Mozer, F. S., Bonnell, J. W., Angelopoulos, V., et al. (2018). Spatial extent and temporal correlation of chorus and hiss: Statistical results from multipoint THEMIS observations. *Journal of Geophysical Research: Space Physics*, 123(10), 8317–8330. <https://doi.org/10.1029/2018JA025725>
- Baker, D. N., Jaynes, A. N., Li, X., Henderson, M. G., Kanekal, S. G., Reeves, G. D., et al. (2014). Gradual diffusion and punctuated phase space density enhancements of highly relativistic electrons: Van Allen Probes observations. *Geophysical Research Letters*, 41(5), 1351–1358. <https://doi.org/10.1002/2013GL058942>
- Bortnik, J., Chen, L., Li, W., Thorne, R. M., & Horne, R. B. (2011). Modeling the evolution of chorus waves into plasmaspheric hiss. *Journal of Geophysical Research*, 116(A8), A08221. <https://doi.org/10.1029/2011JA016499>
- Bortnik, J., Chen, L., Li, W., Thorne, R. M., Nishimura, Y., Angelopoulos, V., & Kletzing, C. A. (2016). Relationship between chorus and plasmaspheric hiss waves. In A. Keiling, D.-H. Lee, & V. Nakariakov (Eds.), *Low-frequency waves in space plasmas*. <https://doi.org/10.1002/9781119055006.ch6>
- Bortnik, J., Inan, U. S., & Bell, T. F. (2006). Landau damping and resultant unidirectional propagation of chorus waves. *Geophysical Research Letters*, 33(3), L03102. <https://doi.org/10.1029/2005GL024553>
- Bortnik, J., Li, W., Thorne, R. M., Angelopoulos, V., Cully, C., Bonnell, J., et al. (2009). An observation linking the origin of plasmaspheric hiss to discrete chorus emission. *Science*, 324(5928), 775–778. <https://doi.org/10.1126/science.1171273>
- Bortnik, J., Thorne, R. M., & Meredith, N. P. (2008). The unexpected origin of plasmaspheric hiss from discrete chorus emissions. *Nature*, 452(7183), 62–66. <https://doi.org/10.1038/nature06741>
- Breneman, A. W., Halford, A., Millan, R., McCarthy, M., Fennell, J., Sample, J., et al. (2015). Global-scale coherence modulation of radiation-belt electron loss from plasmaspheric hiss. *Nature*, 523(7559), 193–195. <https://doi.org/10.1038/nature14515>
- Burtis, W., & Helliwell, R. (1976). Magnetospheric chorus: Occurrence patterns and normalized frequency. *Planetary and Space Science*, 24(11), 1007–1024. [https://doi.org/10.1016/0032-0633\(76\)90119-7](https://doi.org/10.1016/0032-0633(76)90119-7)
- Burtis, W. J., & Helliwell, R. A. (1969). Banded chorus-A new type of VLF radiation observed in the magnetosphere by OGO 1 and OGO 3. *Journal of Geophysical Research*, 74(11), 3002–3010. <https://doi.org/10.1029/JA074i011p03002>
- Chen, L., Bortnik, J., Li, W., Thorne, R. M., & Horne, R. B. (2012b). Modeling the properties of plasmaspheric hiss: 1. Dependence on chorus wave emission. *Journal of Geophysical Research*, 117(A5), A05201. <https://doi.org/10.1029/2011JA017201>
- Chen, L., Bortnik, J., Li, W., Thorne, R. M., & Horne, R. B. (2012c). Modeling the properties of plasmaspheric hiss: 2. Dependence on the plasma density distribution. *Journal of Geophysical Research*, 117(A5), A05202. <https://doi.org/10.1029/2011JA017202>
- Chen, L., Bortnik, J., Thorne, R. M., Horne, R. B., & Jordanova, V. K. (2009). Three-dimensional ray tracing of VLF waves in a magnetospheric environment containing a plasmaspheric plume. *Geophysical Research Letters*, 36(22), L22101. <https://doi.org/10.1029/2009GL040451>
- Chen, L., Li, W., Bortnik, J., & Thorne, R. M. (2012a). Amplification of whistler-mode hiss inside the plasmasphere. *Geophysical Research Letters*, 39(8), L08111. <https://doi.org/10.1029/2012GL051488>
- Chen, L., Thorne, R. M., Bortnik, J., Li, W., Horne, R. B., Reeves, G. D., et al. (2014). Generation of unusually low frequency plasmaspheric hiss. *Geophysical Research Letters*, 41(16), 5702–5709. <https://doi.org/10.1002/2014GL060628>
- Chum, J., & Santolik, O. (2005). Propagation of whistler-mode chorus to low altitudes: Divergent ray trajectories and ground accessibility. *Annales Geophysicae*, 23(12), 3727–3738. <https://doi.org/10.5194/angeo-23-3727-2005>
- Church, S. R., & Thorne, R. M. (1983). On the origin of plasmaspheric hiss: Ray path integrated amplification. *Journal of Geophysical Research*, 88(A10), 7941–7957. <https://doi.org/10.1029/JA088iA10p07941>
- Draganov, A. B., Inan, U. S., Sonwalkar, V. S., & Bell, T. F. (1992). Magnetospherically reflected whistlers as a source of plasmaspheric hiss. *Geophysical Research Letters*, 19(3), 233–236. <https://doi.org/10.1029/91GL03167>

- Dunckel, N., & Helliwell, R. A. (1969). Whistler mode emissions on the Ogo 1 satellite. *Journal of Geophysical Research*, 74(26), 6371–6385. <https://doi.org/10.1029/JA074i026p06371>
- Falkowski, B. J., Tsurutani, B. T., Lakhina, G. S., & Pickett, J. S. (2017). Two sources of dayside intense, quasi-coherent plasmaspheric hiss: A new mechanism for the slot region? *Journal of Geophysical Research: Space Physics*, 122(2), 1643–1657. <https://doi.org/10.1002/2016JA023289>
- Finlay, C., Maus, S., Beggan, C. D., Hamoudi, M., Lowes, F. J., Olsen, N., & Thebaud, E. (2010). Evaluation of candidate geomagnetic field models for IGRF-11. *Earth Planets and Space*, 62(10), 787–804. <https://doi.org/10.5047/eps.2010.11.005>
- Green, J. L., Boardsen, S., Garcia, L., Fung, S. F., & Reinisch, B. W. (2006). Reply to ‘Comment on ‘On the origin of whistler mode radiation in the plasmasphere’ by Green et al. *Journal of Geophysical Research*, 111(A9), A09211. <https://doi.org/10.1029/2006JA011622>
- Green, J. L., Boardsen, S., Garcia, L., Taylor, W. W. L., Fung, S. F., & Reinisch, B. W. (2005). On the origin of whistler mode radiation in the plasmasphere. *Journal of Geophysical Research*, 110(A3), A03201. <https://doi.org/10.1029/2004JA010495>
- Hartley, D. P., Kletzing, C. A., Chen, L., Horne, R. B., & Santolik, O. (2019). Van Allen Probes observations of chorus wave vector orientations: Implications for the chorus-to-hiss mechanism. *Geophysical Research Letters*, 46(5), 2337–2346. <https://doi.org/10.1029/2019GL082111>
- He, Z., Chen, L., Liu, X., Zhu, H., Liu, S., Gao, Z., & Cao, Y. (2019). Local generation of high-frequency plasmaspheric hiss observed by Van Allen Probes. *Geophysical Research Letters*, 46(3), 1141–1148. <https://doi.org/10.1029/2018GL081578>
- He, Z., Yu, J., Chen, L., Xia, Z., Wang, W., Li, K., & Cui, J. (2020). Statistical study on locally generated high-frequency plasmaspheric hiss and its effect on suprathermal electrons: Van Allen Probes observation and quasi-linear simulation. *Journal of Geophysical Research: Space Physics*, 125(10), e2020JA028526. <https://doi.org/10.1029/2020JA028526>
- He, Z., Yu, J., Li, K., Liu, N., Chen, Z., & Cui, J. (2021). A comparative study on the distributions of incoherent and coherent plasmaspheric hiss. *Geophysical Research Letters*, 48(7), e2021GL092902. <https://doi.org/10.1029/2021GL092902>
- Hospodarsky, G. B. (2016). Spaced-based search coil magnetometers. *Journal of Geophysical Research: Space Physics*, 121(12), 12068–12079. <https://doi.org/10.1002/2016JA022565>
- Kennel, C. F., & Petschek, H. E. (1966). Limit on stable trapped particle fluxes. *Journal of Geophysical Research*, 71, 1–28. <https://doi.org/10.1029/JZ071i001p00001>
- Kletzing, C. A., Kurth, W. S., Acuna, M., MacDowall, R. J., Torbert, R. B., Averkamp, T., et al. (2013). The electric and magnetic field instrument suite and integrated science (EMFISIS) on RBSP. *Space Science Reviews*, 179(1–4), 127–181. <https://doi.org/10.1007/s11214-013-9993-6>
- Kurth, W. S., De Pascuale, S., Faden, J. B., Kletzing, C. A., Hospodarsky, G. B., Thaller, S., & Wygant, J. R. (2015). Electron densities inferred from plasma wave spectra obtained by the Waves instrument on Van Allen Probes. *Journal of Geophysical Research: Space Physics*, 120(2), 904–914. <https://doi.org/10.1002/2014JA020857>
- Lam, M. M., Horne, R. B., Meredith, N. P., & Glauert, S. A. (2007). Modeling the effects of radial diffusion and plasmaspheric hiss on outer radiation belt electrons. *Geophysical Research Letters*, 34(20), L20112. <https://doi.org/10.1029/2007GL031598>
- Lam, M. M., Horne, R. B., Meredith, N. P., Glauert, S. A., Moffat-Griffin, T., & Green, J. C. (2010). Origin of energetic electron precipitation >30 keV into the atmosphere. *Journal of Geophysical Research*, 115(A4), A00F08. <https://doi.org/10.1029/2009JA014619>
- Li, J., Bortnik, J., An, X., Li, W., Angelopoulos, V., Thorne, R. M., et al. (2019). Origin of two-band chorus in the radiation belt of Earth. *Nature Communications*, 10(1), 4672. <https://doi.org/10.1038/s41467-019-12561-3>
- Li, W., Chen, L., Bortnik, J., Thorne, R. M., Angelopoulos, V., Kletzing, C. A., et al. (2015). First evidence for chorus at a large geocentric distance as a source of plasmaspheric hiss: Coordinated THEMIS and Van Allen Probes observation. *Geophysical Research Letters*, 42(2), 241–248. <https://doi.org/10.1002/2014GL028332>
- Li, W., & Hudson, M. K. (2019). Earth's Van Allen radiation belts: From discovery to the Van Allen Probes era. *Journal of Geophysical Research: Space Physics*, 124(11), 8319–8351. <https://doi.org/10.1029/2018JA025940>
- Li, W., Ma, Q., Thorne, R. M., Bortnik, J., Kletzing, C. A., Kurth, W. S., et al. (2015a). Statistical properties of plasmaspheric hiss derived from Van Allen Probes data and their effects on radiation belt electron dynamics. *Journal of Geophysical Research: Space Physics*, 120(5), 3393–3405. <https://doi.org/10.1002/2015JA021048>
- Li, W., Thorne, R. M., Bortnik, J., Reeves, G. D., Kletzing, C. A., Kurth, W. S., et al. (2013). An unusual enhancement of low-frequency plasmaspheric hiss in the outer plasmasphere associated with substorm-injected electrons. *Geophysical Research Letters*, 40(15), 3798–3803. <https://doi.org/10.1002/grl.50787>
- Liu, X., Chen, L., & Xia, Z. (2020). The relation between electron cyclotron harmonic waves and plasmopause: Case and statistical studies. *Geophysical Research Letters*, 47(9), e2020GL087365. <https://doi.org/10.1029/2020GL087365>
- Lyons, L. R., & Thorne, R. M. (1973). Equilibrium structure of radiation belt electrons. *Journal of Geophysical Research*, 78(13), 2142–2149. <https://doi.org/10.1029/JA078i013p02142>
- Lyons, L. R., Thorne, R. M., & Kennel, C. F. (1972). Pitch-angle diffusion of radiation belt electrons within the plasmasphere. *Journal of Geophysical Research*, 77(19), 3455–3474. <https://doi.org/10.1029/JA077i019p03455>
- Ma, Q., Li, W., Thorne, R. M., Bortnik, J., Kletzing, C. A., Kurth, W. S., & Hospodarsky, G. B. (2016). Electron scattering by magnetosonic waves in the inner magnetosphere. *Journal of Geophysical Research: Space Physics*, 121(1), 274–285. <https://doi.org/10.1002/2015JA021992>
- Malaspina, D. M., Jaynes, A. N., Boule, C., Bortnik, J., Thaller, S. A., Ergun, R. E., et al. (2016). The distribution of plasmaspheric hiss wave power with respect to plasmopause location. *Geophysical Research Letters*, 43(15), 7878–7886. <https://doi.org/10.1002/2016GL069982>
- Malaspina, D. M., Jaynes, A. N., Hospodarsky, G., Bortnik, J., Ergun, R. E., & Wygant, J. (2017). Statistical properties of low-frequency plasmaspheric hiss. *Journal of Geophysical Research: Space Physics*, 122(8), 8340–8352. <https://doi.org/10.1002/2017JA024328>
- Mauk, B. H., Fox, N. J., Kanekal, S. G., Kessel, R. L., Sibeck, D. G., & Ukhorskiy, A. (2013). Science objectives and rationale for the Radiation Belt Storm Probes Mission. *Space Science Reviews*, 179(1–4), 3–27. <https://doi.org/10.1007/s11214-012-9908-y>
- Meredith, N. P., Bortnik, J., Horne, R. B., Li, W., & Shen, X. (2021). Statistical investigation of the frequency dependence of the chorus source mechanism of plasmaspheric hiss. *Geophysical Research Letters*, 48(6), e2021GL092725. <https://doi.org/10.1029/2021GL092725>
- Meredith, N. P., Horne, R. B., Thorne, R. M., Summers, D., & Anderson, R. R. (2004). Substorm dependence of plasmaspheric hiss. *Journal of Geophysical Research*, 109(A6), A06209. <https://doi.org/10.1029/2004JA010387>
- Meredith, N. P., Horne, R. B., Bortnik, J., Thorne, R. M., Chen, L., Li, W., & Sicard-Piet, A. (2013). Global statistical evidence for chorus as the embryonic source of plasmaspheric hiss. *Geophysical Research Letters*, 40(12), 2891–2896. <https://doi.org/10.1002/grl.50593>
- Meredith, N. P., Horne, R. B., Clilverd, M. A., Horsfall, D., Thorne, R. M., & Anderson, R. R. (2006). Origins of plasmaspheric hiss. *Journal of Geophysical Research*, 111(A9), A09217. <https://doi.org/10.1029/2006JA011707>
- Meredith, N. P., Horne, R. B., Glauert, S. A., & Anderson, R. R. (2007). Slot region electron loss timescales due to plasmaspheric hiss and lightning generated whistlers. *Journal of Geophysical Research*, 112(A8), A08214. <https://doi.org/10.1029/2006JA012413>
- Meredith, N. P., Horne, R. B., Glauert, S. A., Thorne, R. M., Summers, D., Albert, J. M., & Anderson, R. R. (2006). Energetic outer zone electron loss timescales during low geomagnetic activity. *Journal of Geophysical Research*, 111(A5), A05212. <https://doi.org/10.1029/2005JA011516>

- Meredith, N. P., Horne, R. B., Sicard-Piet, A., Boscher, D., Yearby, K. H., Li, W., & Thorne, R. M. (2012). Global model of lower band and upper band chorus from multiple satellite observations. *Journal of Geophysical Research*, *117*(A10), A10225. <https://doi.org/10.1029/2012JA017978>
- Moldwin, M. B., Downward, L., Rassoul, H. K., Amin, R., & Anderson, R. R. (2002). A new model of the location of the plasmapause: CRRES results. *Journal of Geophysical Research*, *107*(A11), 1339. <https://doi.org/10.1029/2001JA009211>
- Nakamura, S., Omura, Y., & Summers, D. (2018). Fine structure of whistler mode hiss in plasmaspheric plumes observed by the Van Allen Probes. *Journal of Geophysical Research: Space Physics*, *123*(11), 9055–9064. <https://doi.org/10.1029/2018JA025803>
- Ni, B., Bortnik, J., Thorne, R. M., Ma, Q., & Chen, L. (2013). Resonant scattering and resultant pitch angle evolution of relativistic electrons by plasmaspheric hiss. *Journal of Geophysical Research: Space Physics*, *118*(12), 7740–7751. <https://doi.org/10.1002/2013JA019260>
- Ni, B., Huang, H., Zhang, W., Gu, X., Zhao, H., Li, X., et al. (2019). Parametric sensitivity of the formation of reversed electron energy spectrum caused by plasmaspheric hiss. *Geophysical Research Letters*, *46*(8), 4134–4143. <https://doi.org/10.1029/2019GL082032>
- Ni, B., Li, W., Thorne, R. M., Bortnik, J., Ma, Q., Chen, L., et al. (2014). Resonant scattering of energetic electrons by unusual low-frequency hiss. *Geophysical Research Letters*, *41*(6), 1854–1861. <https://doi.org/10.1002/2014GL059389>
- Ni, B., & Summers, D. (2010). Resonance zones for electron interaction with plasma waves in the Earth's dipole magnetosphere. I. Evaluation for field-aligned chorus, hiss, and electromagnetic ion cyclotron waves. *Physics of Plasmas*, *17*(4), 042902. <https://doi.org/10.1063/1.3310834>
- Olson, W. P., & Pfizter, K. (1977). Magnetospheric magnetic field modelling. Annual Scientific Report, AFOSR Contract No. F44620–75-c-0033.
- Ripoll, J.-F., Thaller, S. A., Hartley, D. P., Cunningham, G. S., Pierrard, V., Kurth, W. S., et al. (2022). Statistics and empirical models of the plasmasphere boundaries from the Van Allen Probes for radiation belt physics. *Geophysical Research Letters*, *49*(21), e2022GL101402. <https://doi.org/10.1029/2022GL101402>
- Rodger, C. J., & Clilverd, M. A. (2008). Magnetospheric physics: Hiss from the chorus. *Nature*, *452*(7183), 41–42. <https://doi.org/10.1038/452041a>
- Russell, C. T., Holzer, R. E., & Smith, E. J. (1969). OGO 3 observations of ELF noise in the magnetosphere: 1. Spatial extent and frequency of occurrence. *Journal of Geophysical Research*, *74*, 755–777. <https://doi.org/10.1029/JA074i003p00755>
- Santolik, O., & Chum, J. (2009). The origin of plasmaspheric hiss. *Science*, *324*(5928), 729–730. <https://doi.org/10.1126/science.1172878>
- Santolik, O., Chum, J., Parrot, M., Gurnett, D. A., Pickett, J. S., & Cornilleau-Wehrin, N. (2006). Propagation of whistler mode chorus to low altitudes: Spacecraft observations of structured ELF hiss. *Journal of Geophysical Research*, *111*(A10), A10208. <https://doi.org/10.1029/2005JA011462>
- Santolik, O., Kolmasova, I., Pickett, J. S., & Gurnett, D. A. (2021). Multi-point observation of hiss emerging from lightning whistlers. *Journal of Geophysical Research: Space Physics*, *126*(12), e2021JA029524. <https://doi.org/10.1029/2021JA029524>
- Santolik, O., Parrot, M., & Lefeuvre, F. (2003). Singular value decomposition methods for wave propagation analysis. *Radio Science*, *38*(1), 1010. <https://doi.org/10.1029/2000RS002523>
- Sheeley, B. W., Moldwin, M. B., Rassoul, H. K., & Anderson, R. R. (2001). An empirical plasmasphere and trough density model: CRRES observations. *Journal of Geophysical Research*, *106*(A11), 25631–25641. <https://doi.org/10.1029/2000JA000286>
- Shi, R., Li, W., Ma, Q., Reeves, G. D., Kletzing, C. A., Kurth, W. S., et al. (2017). Systematic evaluation of low-frequency hiss and energetic electron injections. *Journal of Geophysical Research: Space Physics*, *122*(10), 10263–10274. <https://doi.org/10.1002/2017JA024571>
- Shprits, Y. Y., Subbotin, D. A., Meredith, N. P., & Elkington, S. R. (2008). Review of modeling of losses and sources of relativistic electrons in the outer radiation belt II: Local acceleration and loss. *Journal of Atmospheric and Solar-Terrestrial Physics*, *70*(14), 1694–1713. <https://doi.org/10.1016/j.jastp.2008.06.014>
- Smith, E. J., Frandsen, A. M. A., Tsurutani, B. T., Thorne, R. M., & Chan, K. W. (1974). Plasmaspheric hiss intensity variations during magnetic storms. *Journal of Geophysical Research*, *79*(16), 2507–2510. <https://doi.org/10.1029/JA079i016p02507>
- Sonwalkar, V. S., & Inan, U. S. (1989). Lightning as an embryonic source of VLF hiss. *Journal of Geophysical Research*, *94*(A6), 6986–6994. <https://doi.org/10.1029/JA094iA06p06986>
- Summers, D., Ni, B., & Meredith, N. P. (2007a). Timescales for radiation belt electron acceleration and loss due to resonant wave-particle interactions: 1. Theory. *Journal of Geophysical Research*, *112*(A4), A04206. <https://doi.org/10.1029/2006JA011801>
- Summers, D., Ni, B., & Meredith, N. P. (2007b). Timescales for radiation belt electron acceleration and loss due to resonant wave-particle interactions: 2. Evaluation for VLF chorus, ELF hiss, and electromagnetic ion cyclotron waves. *Journal of Geophysical Research*, *112*(A4), A04207. <https://doi.org/10.1029/2006JA011993>
- Summers, D., Ni, B., Meredith, N. P., Horne, R. B., Thorne, R. M., Moldwin, M. B., & Anderson, R. R. (2008). Electron scattering by whistler-mode ELF hiss in plasmaspheric plumes. *Journal of Geophysical Research*, *113*(A4), A04219. <https://doi.org/10.1029/2007JA012678>
- Summers, D., Omura, Y., Nakamura, S., & Kletzing, C. A. (2014). Fine structure of plasmaspheric hiss. *Journal of Geophysical Research: Space Physics*, *119*(11), 9134–9149. <https://doi.org/10.1002/2014JA020437>
- Thorne, R. M. (2010). Radiation belt dynamics: The importance of wave-particle interactions. *Geophysical Research Letters*, *37*(22), L22107. <https://doi.org/10.1029/2010GL044990>
- Thorne, R. M., Church, S. R., & Gorney, D. J. (1979). On the origin of plasmaspheric hiss-The importance of wave propagation and the plasmapause. *Journal of Geophysical Research*, *84*(A9), 5241–5247. <https://doi.org/10.1029/JA084iA09p05241>
- Thorne, R. M., Horne, R. B., & Meredith, N. P. (2006). Comment on “On the origin of whistler mode radiation in the plasmasphere” by Green et al. *Journal of Geophysical Research*, *111*(A9), A09210. <https://doi.org/10.1029/2005JA011477>
- Thorne, R. M., Smith, E. J., Burton, R. K., & Holzer, R. E. (1973). Plasmaspheric hiss. *Journal of Geophysical Research*, *78*(10), 1581–1595. <https://doi.org/10.1029/JA078i010p01581>
- Tsurutani, B. T., Falkowski, B. J., Pickett, J. S., Santolik, O., & Lakhina, G. S. (2015). Plasmaspheric hiss properties: Observations from polar. *Journal of Geophysical Research*, *120*(1), 414–431. <https://doi.org/10.1002/2014JA020518>
- Tsurutani, B. T., Falkowski, B. J., Verkhoglyadova, O. P., Pickett, J. S., Santolik, O., & Lakhina, G. S. (2012). Dayside ELF electromagnetic wave survey: A polar statistical study of chorus and hiss. *Journal of Geophysical Research*, *117*(A9), A00L12. <https://doi.org/10.1029/2011JA017180>
- Tsurutani, B. T., Park, S. A., Falkowski, B. J., Bortnik, J., Lakhina, G. S., Sen, A., et al. (2019). Low frequency ($f < 200$ Hz) polar plasmaspheric hiss: Coherent and intense. *Journal of Geophysical Research: Space Physics*, *124*(12), 10063–10084. <https://doi.org/10.1029/2019JA027102>
- Tsurutani, B. T., & Smith, E. J. (1974). Postmidnight chorus: A substorm phenomenon. *Journal of Geophysical Research*, *79*(1), 118–127. <https://doi.org/10.1029/JA079i001p00118>
- Tsurutani, B. T., & Smith, E. J. (1977). Two types of magnetospheric ELF chorus and their substorm dependences. *Journal of Geophysical Research*, *82*(32), 5112–5128. <https://doi.org/10.1029/JA082i032p05112>
- Tsurutani, B. T., Smith, E. J., & Thorne, R. M. (1975). Electromagnetic hiss and relativistic electron losses in the inner zone. *Journal of Geophysical Research*, *80*(4), 600–607. <https://doi.org/10.1029/JA080i004p0600>
- Tsurutani, B. T., Smith, E. J., West, H. I., & Buck, R. M. (1979). Chorus, energetic electrons and magnetospheric substorms. In P. J. Palmadesso, & K. Papadopoulos (Eds.), *Wave instabilities in space plasmas*. https://doi.org/10.1007/978-94-009-9500-0_6

- Tsurutani, B. T., & Thorne, R. M. (1982). Diffusion processes in the magnetopause boundary layer. *Geophysical Research Letters*, *9*(11), 1247–1250. <https://doi.org/10.1029/GL009i011p01247>
- Tsurutani, B. T., Verkhoglyadova, O. P., Lakhina, G. S., & Yagitani, S. (2009). Properties of dayside outer zone chorus during HILDCAA events: Loss of energetic electrons. *Journal of Geophysical Research*, *114*(A3), A03207. <https://doi.org/10.1029/2008JA013353>
- Van Allen, J. A. (1959). The geomagnetically trapped corpuscular radiation. *Journal of Geophysical Research*, *64*(11), 1683–1689. <https://doi.org/10.1029/JZ064i011p01683>
- Verkhoglyadova, O. P., Tsurutani, B. T., & Lakhina, G. S. (2010). Properties of obliquely propagating chorus. *Journal of Geophysical Research*, *115*(A9), A00F19. <https://doi.org/10.1029/2009JA014809>
- Zhao, H., Ni, B., Li, X., Baker, D. N., Johnston, W. R., Zhang, W., et al. (2019). Plasmaspheric hiss waves generate a reversed energy spectrum of radiation belt electrons. *Nature Physics*, *15*(4), 367–372. <https://doi.org/10.1038/s41567-018-0391-6>
- Zhu, H., Liu, X., & Chen, L. (2019). Triggered plasmaspheric hiss: Rising tone structures. *Geophysical Research Letters*, *46*(10), 5034–5044. <https://doi.org/10.1029/2019GL082688>